International Journal of Remote Sensing, 2013
Vol. 34, No. 16, 5997–6016, http://dx.doi.org/10.1080/01431161.2013.803169

Daily MODIS 500 m reflectance anisotropy direct broadcast (DB) products for monitoring vegetation phenology dynamics

Yanmin Shuai[a]*, Crystal Schaaf[b], Xiaoyang Zhang[c,d], Alan Strahler[e], David Roy[f], Jeffrey Morisette[g], Zhuosen Wang[b], Joanne Nightingale[h], Jaime Nickeson[h], Andrew D. Richardson[i], Donghui Xie[j,k,l], Jindi Wang[j,k,l], Xiaowen Li[j,k,l], Kathleen Strabala[m], and James E. Davies[m]

[a]ERT Inc. at the Biospheric Sciences Laboratory of NASA's Goddard Space Flight Center, Greenbelt, MD 20771, USA; [b]School for the Environment, University of Massachusetts Boston, Boston, MA 02125, USA; [c]Earth System Science Interdisciplinary Center, University of Maryland, College Park, MD, USA; [d]NOAA/NESDIS/STAR, College Park, MD, USA; [e]Center for Remote Sensing, Department of Earth and Environment, Boston University, MA 02215, USA; [f]Geographic Information Science Center of Excellence, South Dakota State University, Brookings, SD 57007, USA; [g]US Geological Survey, DOI North Central Climate Science Center, Fort Collins, CO 80525, USA; [h]Sigma Space Corporation at the Terrestrial Information Systems Laboratory of NASA's Goddard Space Flight Center, Greenbelt, MD 20771, USA; [i]Department of Organismic and Evolutionary Biology, Harvard University, Cambridge, MA 02138, USA; [j]State Key laboratory of Remote Sensing Science, Jointly Sponsored by Beijing Normal University and the Institute of Remote Sensing Applications, Chinese Academy of Sciences, Beijing, China; [k]Beijing Key Laboratory for Remote Sensing of Environment and Digital Cities, Beijing Normal University, Beijing, China; [l]School of Geography and Remote Sensing Science, Beijing Normal University, Beijing 100875, China; [m]Space Science and Engineering Center (SSEC/UW-Madison), Madison, WI 53706, USA

(*Received 20 January 2013; accepted 2 May 2013*)

Land surface vegetation phenology is an efficient bio-indicator for monitoring ecosystem variation in response to changes in climatic factors. The primary objective of the current article is to examine the utility of the daily MODIS 500 m reflectance anisotropy direct broadcast (DB) product for monitoring the evolution of vegetation phenological trends over selected crop, orchard, and forest regions. Although numerous model-fitted satellite data have been widely used to assess the spatio-temporal distribution of land surface phenological patterns to understand phenological process and phenomena, current efforts to investigate the details of phenological trends, especially for natural phenological variations that occur on short time scales, are less well served by remote sensing challenges and lack of anisotropy correction in satellite data sources. The daily MODIS 500 m reflectance anisotropy product is employed to retrieve daily vegetation indices (VI) of a 1 year period for an almond orchard in California and for a winter wheat field in northeast China, as well as a 2 year period for a deciduous forest region in New Hampshire, USA. Compared with the ground records from these regions, the VI trajectories derived from the cloud-free and atmospherically corrected MODIS Nadir BRDF (bidirectional reflectance distribution function) adjusted reflectance (NBAR) capture not only the detailed footprint and principal attributes of the phenological events (such as flowering and blooming) but also the substantial inter-annual variability. This study demonstrates the utility of the daily 500 m MODIS reflectance anisotropy DB product to provide daily VI for monitoring and detecting changes of the natural vegetation

*Corresponding author. Email: Yanmin.Shuai@nasa.gov

phenology as exemplified by study regions comprising winter wheat, almond trees, and deciduous forest.

1. Introduction

Land surface phenology, defined as the seasonal pattern of variation in vegetated land surfaces characterized by satellite remote sensing products (Jolly, Nemani, and Running 2005; Zhang, Friedl, and Schaaf 2006), is an efficient bio-indicator for monitoring terrestrial ecosystem variation in response to changing climatic factors. Changes in phenological events are increasingly being seen as important signals of year-to-year climatic variations or even global environmental changes, and phenological studies are being used to monitor the impact of climate change on individual species at a number of scales (Reed et al. 1994; Schwartz, Ahas, and Aasa 2006; Cleland et al. 2007). The timing of leaf development in many temperate deciduous species correlates with cumulative springtime temperatures (Cannell and Smith 1983; Rötzer, Grote, and Pretzsch 2004; Zhang and Goldberg 2010; Zhang, Goldberg, and Yu 2012). The length of growing season may strongly affect the associated seasonality of ecosystem-scale carbon exchange, especially in deciduous forests (White, Running, and Thornton 1999; White et al. 2009; Richardson, Braswell, et al. 2009, 2010, 2012). A number of studies have linked vegetation's response via phenology and length of regional growing seasons with climatic and ecological changes (e.g. Myneni et al. 1997; Parmesan and Yohe 2003; Liang and Schwartz 2009; Liang, Schwartz, and Fei 2012). Conversely, various studies show vegetation's feedback on local climate via biochemical and biophysical processes. Temperature is the main factor controlling the seasonality of vegetation growth in humid temperate climates (Schwartz 1998; Zhang et al. 2004), and water availability governs vegetation phenology in arid and semiarid ecosystems and in seasonally dry tropical climates (Justiniano and Fredericksen 2000; Kramer, Leinomen, and Loustau 2000; Zhang et al. 2010) where rainfall activates the emergence of green leaves and controls the duration of vegetation growth (Spano et al. 1999; Cook and Heerdegen 2001). The pattern of precipitation during rainy seasons is critical to crop germination, growth, and harvest (e.g. Lobell and Field 2007; Osborne et al. 2007; Omotosho 1992), and the early or late arrival of precipitation events can affect estimations of agriculture growth and yield.

Many land surface phenology investigations have been devoted to the development of various methods (de Beurs and Henebry 2010) for identifying and calculating phenological features using time series of vegetation indices (VIs). A regression-based model of first leaf emergence is used to detect the onset of spring (Schwartz 1990). User-defined thresholds depending on land cover types are adopted to identify the phenological dates (White, Thornton, and Running 1997; White et al. 2002; Schwartz, Reed, and White 2002). In most recent studies, phenological time series are explored using the TIMESAT smoothing algorithm (Jonsson and Eklundh 2004; Tan et al. 2011) to fill gaps and reduce noise in the satellite signal, through a complex six-parameter model to fit sparse greenness profiles (Badhwar 1984), and also through piecewise logistic functions to determine onset dates (Zhang et al. 2003; Ganguly et al. 2010). These methods have significantly improved our understanding of spatial phenological patterns (Zhang and Goldberg 2010), the link between climate change and ecosystem variations (Busetto et al. 2010), and the contribution of forest phenology to the estimation of carbon flux (Jenkins et al. 2007). On the other hand, fitted or smoothed phenological time series over multi-day composite products can mask high-frequency vegetation changes, possibly missing short-term changes evident in crop defoliation, post snowmelt green-up in the Arctic, or fire and other sudden

disturbances (White, Thornton, and Running 1997; White and Nemani 2006; McKellip et al. 2005; Narasimhan and Stow 2010; Ju et al. 2010). As some resource management actions rely on knowing the date of such disturbances as accurately as possible and reacting to the disturbance as quickly as possible afterwards (e.g. replanting when crops fail or reducing erosion after fire), fine-temporal resolution satellite products are required for the exploration and monitoring of land surface vegetation phenological events.

Traditionally, land surface phenological metrics have been extracted from weekly, 10 day, and 14 day NOAA/AVHRR (Advanced Very High Resolution Radiometer) archives (Reed et al. 1994; Schwartz, Reed, and White 2002; de Beurs and Henebry 2008; Kross et al. 2011), and for the past decade from 16 day MODIS operational products (Zhang, Friedl, and Schaaf 2006; Ganguly et al. 2010). Compared with AVHRR, MODIS has seven carefully selected bands for land applications, finer spatial resolution (250 m to 500 m), improved geolocation accuracy (50 m at nadir), systematic atmospheric correction schemes and cloud screening, and upgraded sensor calibration (Justice et al. 1998; Wofle et al. 2002; Box et al. 2006; Heidinger, Cao, and Sullivan 2002). The routine MODIS reflectance anisotropy and albedo products (MCD43) (Schaaf et al. 2002, 2011) use high-quality, multi-spectral, cloud-free, atmospherically corrected surface reflectances from both Terra and Aqua to provide global quantities with the anisotropy correction for directional reflectance at a 500 m spatial resolution every 8 days (based on a 16 day window). While the operational product was originally envisaged as a daily product, archive constraints restricted it to an 8 day retrieval schedule. However, due to the increasing needs of the MODIS direct broadcast (DB) user community, a daily DB algorithm was implemented (Shuai 2010) and released through the University of Wisconsin–Madison Space Science and Engineering Center (SSEC) to more than 125 MODIS DB stations around the world (http://cimss.ssec.wisc.edu/imapp/db_brdf_v1.0.shtml). This package, providing daily 500 m albedo measures and Nadir BRDF (bidirectional reflectance distribution function)-adjusted reflectance (NBAR), is well suited for investigating the natural trajectories of various vegetation species with rapid growth patterns or impacted by frequent disturbances.

In this study, daily MODIS 500 m NBAR-based phenological markers are compared to ground measurements carried out over three homogenous sites (an almond orchard in California, a winter wheat region in northeast China, and a deciduous forest in New Hampshire, USA). More precisely, the primary objective is to explore the utility of daily MODIS-derived NBAR to characterize the VI trajectories of various vegetation species. A secondary objective is to examine the natural phenological changes in the above three vegetation species. A further objective is to maximize the inherent ability of the MODIS DB system by providing the near real-time phenological information on vegetated areas for the pressing requirements in rapid-response systems.

2. Data and methods

2.1. Field data

The first study area (37° 30′ 41.04″ N, 121° 12′ 47.73″ W), located in western Stanislaus County in the northern San Joaquin valley region of central California, USA, is a typical almond orchard with more than 100 acres of continuous rows of mature trees. In such orchards, grass, or planted crops are often found in the understorey vegetation. Since 2001, weather conditions and phenological events related to California almond orchards have been reported based on field observations from numerous growers through the

blue diamond growers website (http://www.bluediamond.com/applications/in-the-field). The regularly scheduled field reports describe the detailed status and evolution of each growth stage from dormant, green tips, buds, blooming, jacketing, to the nuts developing through descriptions and field photos. In this case study, we extracted the phenological dates (Table 1) in terms of the estimated percentage of individuals entering each stage for the 2006 crop year of the selected orchard.

The ground-based crop growth stages for the second site were collected over the Yucheng Experiment Site (YCES) in the agricultural region of the northeast China plain by the Chinese ecosystem research network at YCES. This site, located southwest of Yucheng city at 36.8290°N, 116.5704°E, has been planted with winter wheat and summer corn over 90% of its area since the year 2000. The *in situ* data record used in this case study includes frequent field specification of the surface phenology information during the 2005 growing season. Table 1 summarizes the ground observations of the phenological period available for the winter wheat crops at Yucheng. According to the field criterion, the 'start' of a growth stage means that ∼10% of the individual crops have entered into the growth phase, while the 'end' indicates that ∼90% crops have completed this stage.

The third case study was conducted at the Bartlett Experimental Forest (BEF, 44° 17′ N, 71° 3′ W), located within the Saco Ranger District of the White Mountains National Forest in north-central New Hampshire, USA. The dominant trees are northern hardwood species (*Acer saccharum*, sugar maple; *Fagus grandifolia*, American beech; and *Betula alleghaniensis*, yellow birch) with some red maple, paper birch, and occasionally conifers, such as eastern hemlock (Richardson et al. 2007; Richardson, Hollinger, et al. 2009). A digital webcam mounted near the top of a 26.5 m tower, looking north, and angled slightly downward, has been providing digital images recorded daily between 12:00 and 14:00 hours since 2005 (Jenkins and Richardson et al. 2007; Richardson, Hollinger, et al. 2009; Sonnentag et al. 2012; Hufkens et al. 2012). The main species in the vicinity of the tower are red maple, sugar maple, and American beech. Qualitative information about the autumn foliage colour change stage is summarized in Table 1, and is based on descriptions from ∼600 local spotters for the foliage network (http://www.foliagenetwork.net).

Each of these three sites were selected because of the availability of key field data needed to assess the utility of the DB phenology product, as well as the sites' specific and fairly strong phenology signal. Following the objective of the article, we use these sites to develop a 'proof of concept' for using the DB data for estimating phenology parameters (noting that further work is needed to test and extend the approach to other areas and over time).

2.2. Daily MODIS VI

Both the global MODIS operational and daily DB algorithms utilize the semi-empirical kernel-driven RossThickLiSparse-Reciprocal (RTLSR) model (Roujean, Leroy, and Deschamps 1992; Lucht, Schaaf, and Strahler 2000) to capture the radiative transfer (Ross 1981) scattering and shadowing components (Li and Strahler 1992) of the surface to reconstruct the BRDF at each pixel. This study utilized a daily rolling strategy over a 16 day period, with an emphasis on the most recent high-quality observation in the dynamic input stream by dropping the oldest and adding the newest looks (Lucht and Lewis 2000; Roy et al. 2006; Shuai et al. 2008; Shuai 2010; Ju et al. 2010) to retrieve BRDFs and spectral albedo quantities from high-quality, multi-spectral, cloud-free, atmospherically corrected surface reflectances. Less change will be found on the retrieved BRDF shape if insufficient clear observations are added in the dynamic input stream, especially during the coming

Table 1. The field-based phenological stages for almond orchard (upper left), forest (lower left), and winter wheat (right).

Almond orchard at CA (during 2006-001 to 2006-160)*		
Growth stages	Year-DOY	Date
Dormant	2006-001	1 January 2006
Green tip and pink bud	2006-029	29 January 2006
Popcorn, bloom, and petal fall	2006-042	11 February 2006
Jacket and early nuts developing	2006-067	8 March 2006
Late nuts developing	2006-103	13 April 2006

Mixed forest at Bartlett†		
Foliage colour change	Year-DOY	Date
Little to no change	2005-260	17 September 2005
	2006-252	9 September 2006
Low colour (11–30%)	2005-264	21 September 2005
	2006-256	13 September 2006
Moderate colour (31–60%)	2005-274	1 October 2005
	2006-266	23 September 2006
High colour (61–80%)	2005-281	8 October 2005
	2006-273	30 September 2006
Peak colour (81–100%)	2005-285	12 October 2005
	2006-280	7 October 2006
Past peak and high leaf drop	2005-299	26 October 2005
	2006-287	14 October 2006

Winter wheat (variety #13) at the YCES‡		
Growth stages	Year-DOY	Date
Seeding	2004-284	10 October 2004
Emergence	2004-295	21 October 2004
Tiller	2004-313	8 November 2004
Turning green	2005-074	15 March 2005
Erect growth	2005-081	22 March 2005
First node visible	2005-097	7 April 2005
Boot stage	2005-122	19 April 2005
Heading	2005-109	2 May 2005
Beginning flower	2005-127	7 May 2005
Ripening	2005-132	12 May 2005
Milky ripe	2005-142	22 May 2005
Mealy ripe	2005-157	6 June 2005
Kernel hard	2005-163	12 June 2005
Harvest	2005-166	15 June 2005

Notes: *Data extracted from the description provided by http://www.bluediamond.com/applications/in-th-field; †data extracted from the foliage reports provided by http://www.foliagenetwork.net; ‡ground data collected by the Chinese Ecosystem Research Network at Yucheng Experiment Site (YCES), Chinese Academy of Sciences (CAS), http://www.cern.ac.cn.

continuous cloud days. A full BRDF retrieval was attempted if at least seven cloud-free observations were available during a 16 day period, and these observations adequately sampled the viewing geometry (Lucht, Schaaf, and Strahler 2000; Shuai et al. 2008). Otherwise a poorer-quality magnitude inversion was performed using *a priori* BRDF information. Validation indicates that both full and backup magnitude inversion have a good agreement with the available ground sites (Shuai 2010; Wang et al. 2012). To remove the view angle effect, the NBAR data were normalized into nadir view with the sun at local solar noon in terms of the most recent day of the retrieval period.

We generated a time series of daily NBAR at the local solar noon for each day in the growth period of three vegetation sites. Satellite-based VIs, which provide an indication of canopy greenness, are commonly used to monitor seasonal, inter-annual, and long-term variations in vegetation structural, phenological, and biophysical parameters (Morisette et al. 2009). VIs, spectral transformations of two or more bands, enhance the contribution of vegetation properties and allow reliable spatial and temporal inter-comparisons of vegetation activities, and the normalized difference vegetation index (NDVI, Equation (1)) and enhanced vegetation index (EVI, Equation (2)) are most widely used in vegetation studies (Reed et al. 1994; Myneni et al. 1995; Huete et al. 2002; White et al. 2009; Zhang et al. 2003; Zhang and Goldberg 2010). As values of NDVI and EVI normally vary with sun and view geometry (Moody and Strahler 1994) in the order of 0.05–0.2 (Leroy and Hautecoeur 1999), it is desirable to use view angle-corrected reflectances such as NBAR for consistent comparisons. Therefore, time series of NDVI and EVI for each study site were calculated from the resultant daily MODIS 500 m NBAR for each day in the growth period of winter wheat (2005-060 to 2005-190), the developing bloom period of the almond orchard (2006-001 to 2006-160), and the senescence periods of 2005 and 2006 over the Bartlett forest region (from days 195 to 299).

$$\mathrm{NDVI} = \frac{\rho_{\mathrm{NIR}} - \rho_{\mathrm{red}}}{\rho_{\mathrm{NIR}} + \rho_{\mathrm{red}}}, \tag{1}$$

$$\mathrm{EVI} = G\frac{\rho_{\mathrm{NIR}} - \rho_{\mathrm{red}}}{\rho_{\mathrm{NIR}} + C_1\rho_{\mathrm{red}} - C_2\rho_{\mathrm{blue}} + L}. \tag{2}$$

In the above, ρ represents the nadir view angle-corrected surface reflectance in the MODIS near-infrared (NIR, 841–876 nm), red (620–670 nm), and blue (459–479 nm) bands, L is the adjustment for canopy background, and C_1 and C_2 are the coefficients of the aerosol resistance term. The coefficients adopted in the EVI algorithm are $L = 1$, $C_1 = 6$, $C_2 = 7.5$, and G (gain factor) $= 2.5$ (Huete et al. 2002).

3. Results and discussion

3.1. Bloom detection for the almond orchard

The DB algorithm was used to compute the daily MODIS NBAR-derived VIs (EVI and VI) from the 500 m spectral NBAR over the California almond orchard. The NBAR-VI and NBARs (NIR, red, and green bands) were extracted for one 500 m MODIS pixel (Figure 1), centred over a 30 km by 30 km region (NBAR-EVI, Figure 2), to capture the development of the almond growth stages (Figure 3) over days 1–160 of the 2006 growing season. Both NBAR-NDVI and NBAR-EVI in Figure 1 capture the slow increase in the early growing season (days 20 to ∼40) as the green tips increase, with a significant decrease in NDVI (and

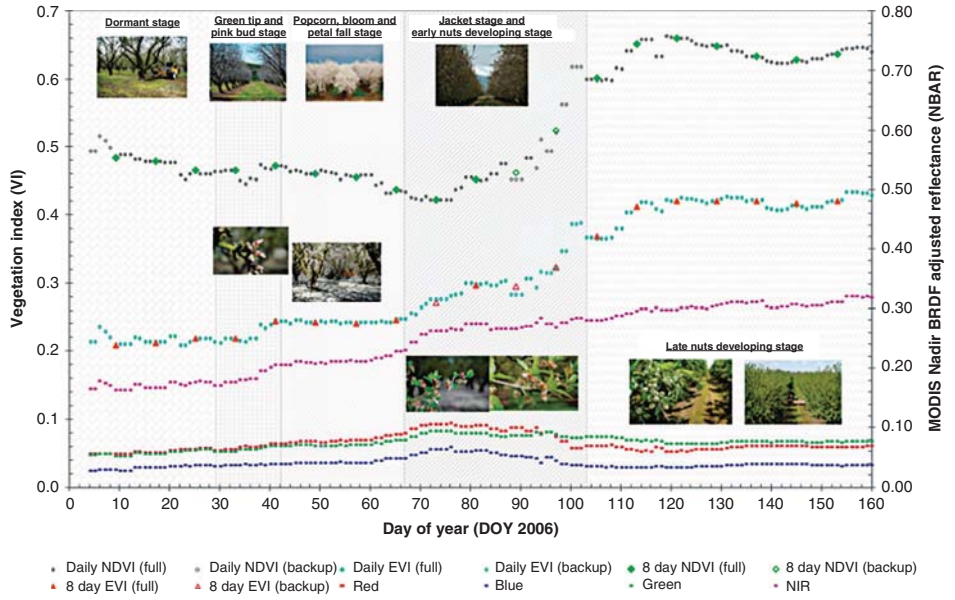

Figure 1. Time series of the 500 m MODIS NBAR-based EVI (cyan) and NDVI (grey) extracted from full inversion (solid dot) and backup magnitude inversions (empty dot), the standard 8 day MODIS NBAR-derived NDVI (green diamond) and EVI (brown triangle), and spectral nadir BRDF adjusted reflectances (NBAR) in red, blue, green, and NIR bands over the almond orchard in the northern San Joaquin Valley region of central California with embedded phenological phases (shaded with watermark backgrounds) and accompanying pictures.

a shallow dip in EVI) occurring during the popcorn bloom–petal fall stage (days ~40–70), followed by a rapid and continuing increase in the jacket stage and the early nut development stage (days 70–110) and a shift to saturated and stable values through the late nut development stage (days ~110–160). The NDVI varies from 0.42 to ~0.68, while the EVI plot, constrained by the blue band, has a lower dynamic range from 0.2 to ~0.45. An increase in understorey in the early growth period, especially in the warm San Joaquin Valley, may contribute more to the increase in NIR and VI values than the development of green tips from the almond trees. A suppression of NIR and a slight increase in red and blue bands coincide with the emergence of pinkish white blossoms (Figure 3). Thus both the NDVI and EVI plots record dips as the blooming stage dominates the field of view of the MODIS sensor, and dip further when the green understorey is obscured by the fallen petals.

The daily MODIS NBAR-EVI regional maps (Figure 2), also calculated by the DB algorithm for days 1–160 of 2006, capture the phenological transition of the larger 30 km by 30 km area centred on the same almond orchard in the northern San Joaquin Valley region of central California. The transition of EVI values in the centre of the region replicates the above pixel analysis, with values varying from ~0.2 to 0.4 from dormant to nut development stage. Two irrigation ditches, winding through the centre region, may however reduce reflectance values of the underlying 500 m pixels. The lower EVI values in the upper left of the region are related to a mountainous area (to the west of route 5-West Side Fwy) that is covered by very sparse herbaceous vegetation. Relatively high EVI values (up to 0.8) are acquired in the lower right of the region, which is covered by a mature almond orchard with the rich understorey of pasture, hay, and cultivated crops in terms of the 30 m

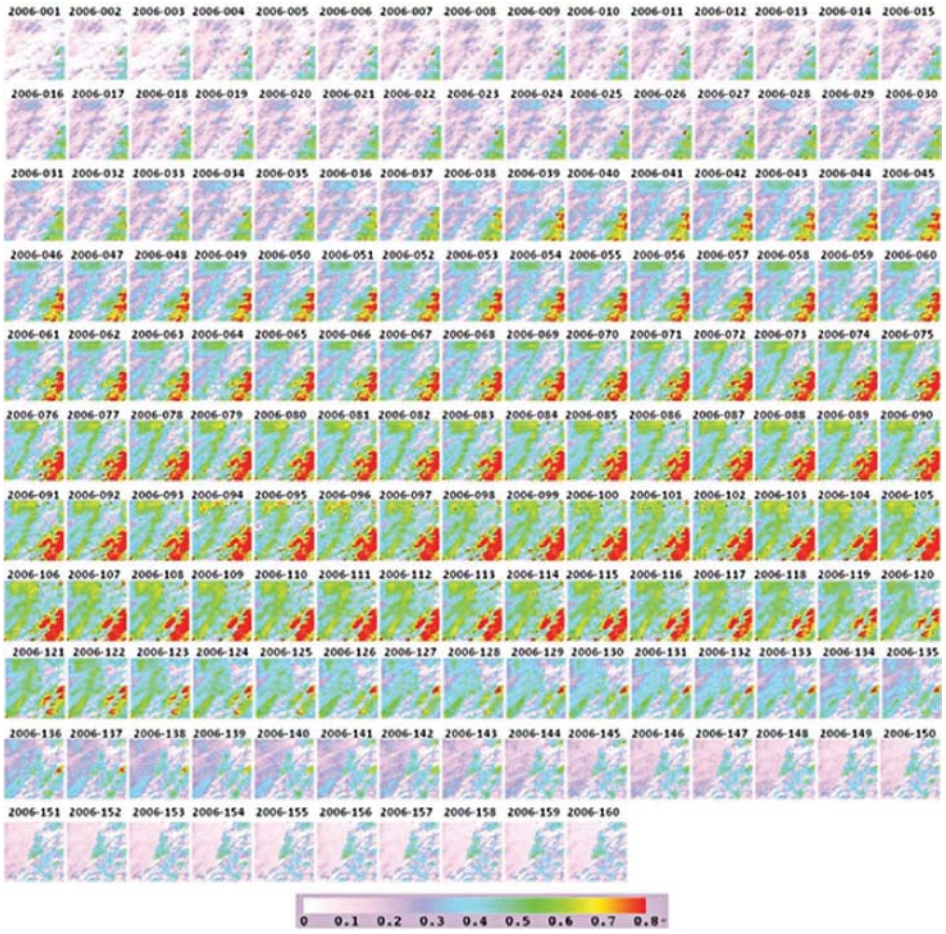

Figure 2. Temporal EVI maps of a 30 km by 30 km region centred on the investigated almond orchard in the northern San Joaquin Valley region of central California for the year 2006, with a mountainous region covered by sparse vegetation at the upper left, various densities of orchards in the middle, and pasture/hay/cultivated crops (in terms of the 30 m NLCD 2006 classification map) at the lower right.

national land cover data (NLCD classification map). These EVI values drop quickly once the understorey green vegetation developed into the senescent period or got harvested after day 130.

3.2. Investigation of the growth phases for winter wheat crops

Figure 4 shows the seasonal winter wheat phenology profiles from the daily 500 m DB MODIS NBAR-derived NDVI and EVI. The dynamic range of the Yucheng site varies from 0.25 to nearly 0.60 for NDVI, and from 0.15 to ~0.45 for EVI. Comparisons with the field-based record of phenology events (Table 1) show that both the MODIS daily DB NBAR-NDVI and EVI captured the main growth features of the winter wheat crop with a rapid green-up from the middle of March to early April, followed by a slower increase after the emergence of the first node. Then the indices reach their highest values during the

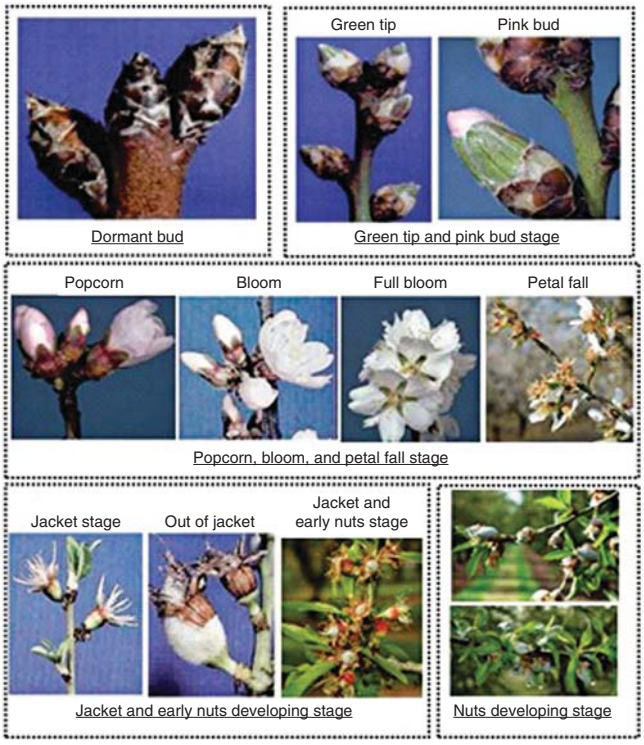

Figure 3. The growth stages of California almond trees from the dormant stage (upper left) to nut development stage (lower right); pictures provided by UC Statewide IPM Project, 2000 Regents, University of California, http://www.ipm.ucdavis.edu/PMG/C003/m003bcwhybloom.html, and http://bluediamond.com/applications/in-the-field.

2 week period of heading and flowering, with a gradual decrease during the ripening period, and a final drop to the harvest season in late June. The daily NBAR VIs in Figure 4 capture some fine details during the periods of rapid change in this growing season. For instance, in the flowering and ripening periods, which were captured with a large number of high-quality full retrievals, the daily VI plots exhibit a shallow dip, particularly in the NBAR-EVI plot. In general wheat flowers are light yellow (see the embedded picture E in Figure 4), which may partly decrease the 'greenness' of the crop, reducing the reflectance in the NIR band and inducing a slight decrease in EVI. When the flowering period is completely over, the NBAR-EVI values rebound slightly.

Figure 5 shows the spatio-temporal variability of daily MODIS NBAR-EVI from days 2005-060 to 2005-191 for a 30 km by 30 km area centred on the Yucheng experimental site. Generally, the time series of the EVI pictures replicate the winter wheat pixel analysis provided in Figure 4, with values varying from $\sim$0.2 to 0.6. The pure white areas in days 60–62 are affected by cloud, and the cluster of pixels with an EVI $<$0.2 located in the upper left is related to the town of Yucheng. These regional images indicate the applicability of field phenology information to the larger local area. Widespread greening occurs across the region between days 79 and 87, while widespread maturity appears from day 120 onwards. Increasing regional senescence was evident from day 143 onwards, and harvest appears to have taken place from day 165 onwards.

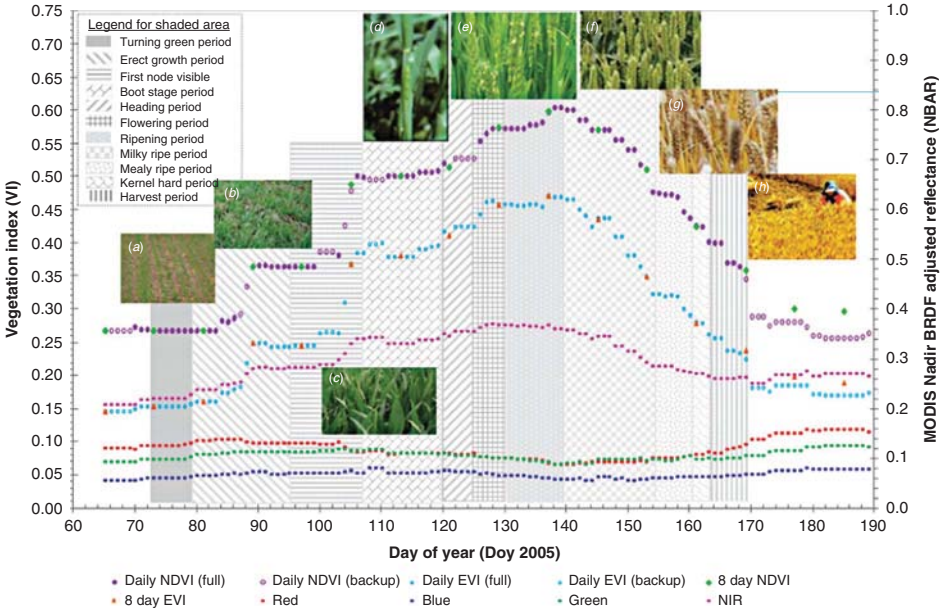

Figure 4. Time series of the 500 m daily MODIS NBAR-derived EVI (cyan) and NDVI (purple) extracted from full inversion (solid dot) and backup magnitude inversions (empty dot), the standard 8 day MODIS NBAR-derived NDVI (green diamond) and EVI (brown triangle), and spectral nadir BRDF adjusted reflectance (NBAR) in red, blue, green, and NIR bands over winter wheat crops at the Yucheng site with embedded phenological phases (shaded with watermark backgrounds) and accompanying pictures (*a*) turning green, (*b*) erect growth, (*c*) first node visible, (*d*) boot stage, (*e*) flowering and ripening, (*f*) ripe period, (*g*) kernel hard period, and (*h*) harvest.

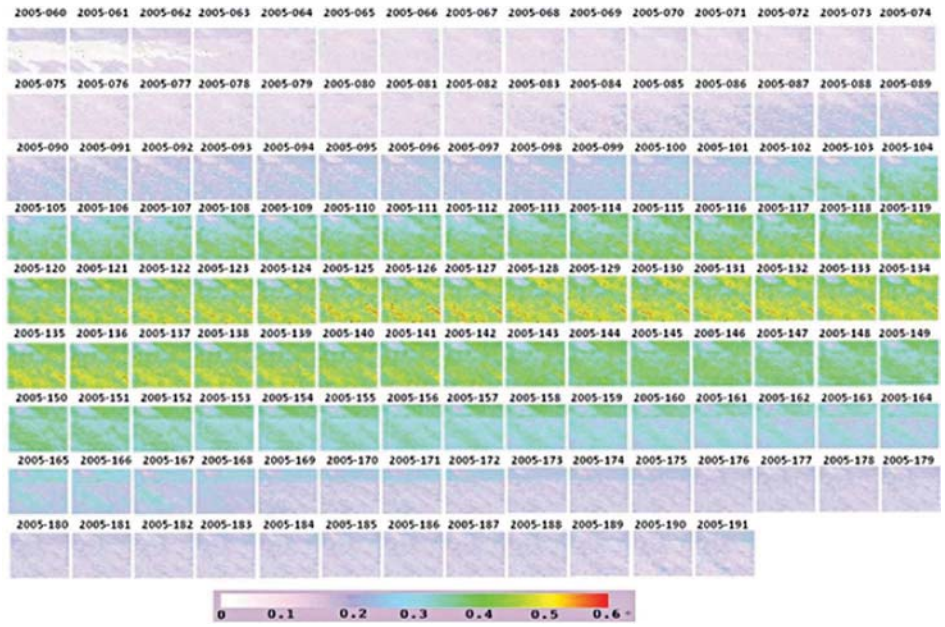

Figure 5. Temporal EVI maps of a 30 km by 30 km region centred on the winter wheat field at YCES during the above-ground growth period for the year 2005.

3.3. Changes in forest senescence

The hardwood forests of northern New Hampshire (and particularly the area near Bartlett, NH) are justly famous for their annual display of autumn colours, with bright yellows and vibrant reds. Figure 6 displays the temporal changes of MODIS NBAR-derived EVI and NDVI over the Bartlett experimental site, and spans the period from vegetation maturity (days 200–220, picture A) through senescence. Senescence, as shown by the EVI plots, started in late August, with a gradually continuous drop, while the diminution of NDVI started in early September. This may be caused by EVI's increased sensitivity to foliage information in dense forest canopies through a de-coupling of the canopy background signal and a reduction in atmospheric and soil reflectance influence (Huete et al. 2002), as the leaves of some forest species are turning more colourful by the end of August. The entire region near the vicinity of the Bartlett tower has undergone senescence by late October (day ~304) as shown in the landscape phenology pictures D and E. Compared with 2005, the autumn senescence in 2006 appears to have begun almost 10 days earlier (day ~264). In 2006, a very strong cold front moved through the area around day 265, bringing heavy rain and up to 31 m s^{-1} strong winds, which broke some branches and trees, and hastened the autumn senescence process of this deciduous forest. Note that the lowest VI values are still higher than 0.5 for NDVI and 0.2 for EVI, as a parcel of predominantly evergreen trees to the far north of the tower (shown in picture B–E) does fall within the MODIS 500 m pixel bin and is also contributing to the VI signal.

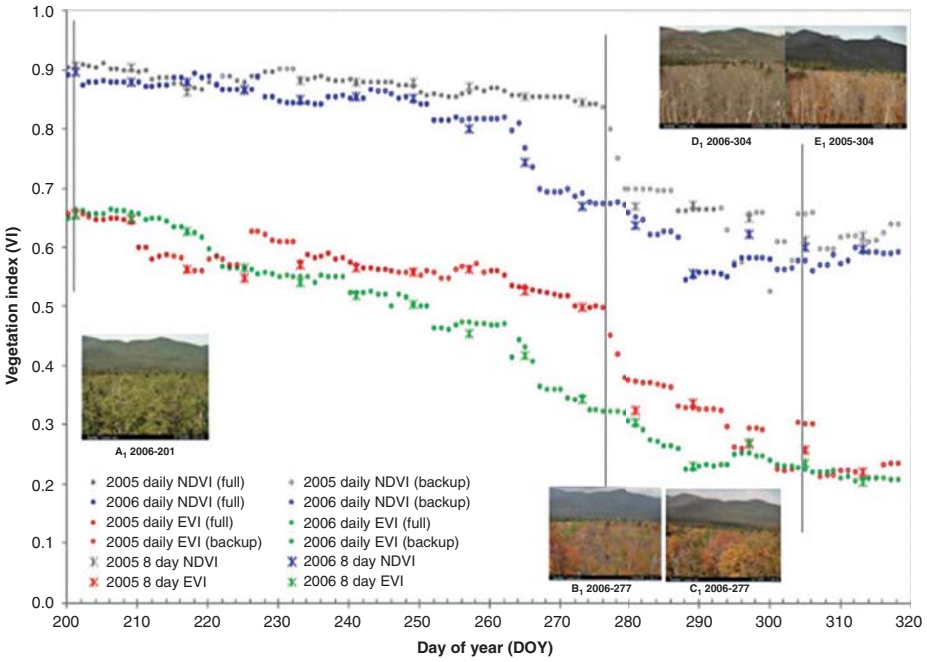

Figure 6. Time series of the 500 m MODIS NBAR-derived NDVI (grey for 2005 and blue for 2006), EVI (red for 2005 and green for 2006) extracted from full (solid dot) and backup magnitude inversions (empty dot), and the standard 8 day NBAR-derived vegetation indices (stars) over the mixed forest at Bartlett site with the embedded ground landscape phenology photos taken by Bartlett webcam (lower pictures A–E).

Figure 7 shows the temporal 30 km by 30 km regional subsets of EVI extracted from MODIS-derived NBAR at local solar noon and centred on the Bartlett tower location from days 195 to 299 for the years 2005 (upper picture) and 2006 (lower picture). The daily regional NBAR-EVIs are used to track the transition of the photosynthetically active green deciduous foliage from the thick canopy cover (high EVI values) into the vivid reds, yellows, and browns of autumn senescence. Again it is clear that the senescence in the region occurred quite a few days later in 2005 than in 2006. This is further verified by the report from the foliage network (http://www.foliagenetwork.net), which indicated that the foliage

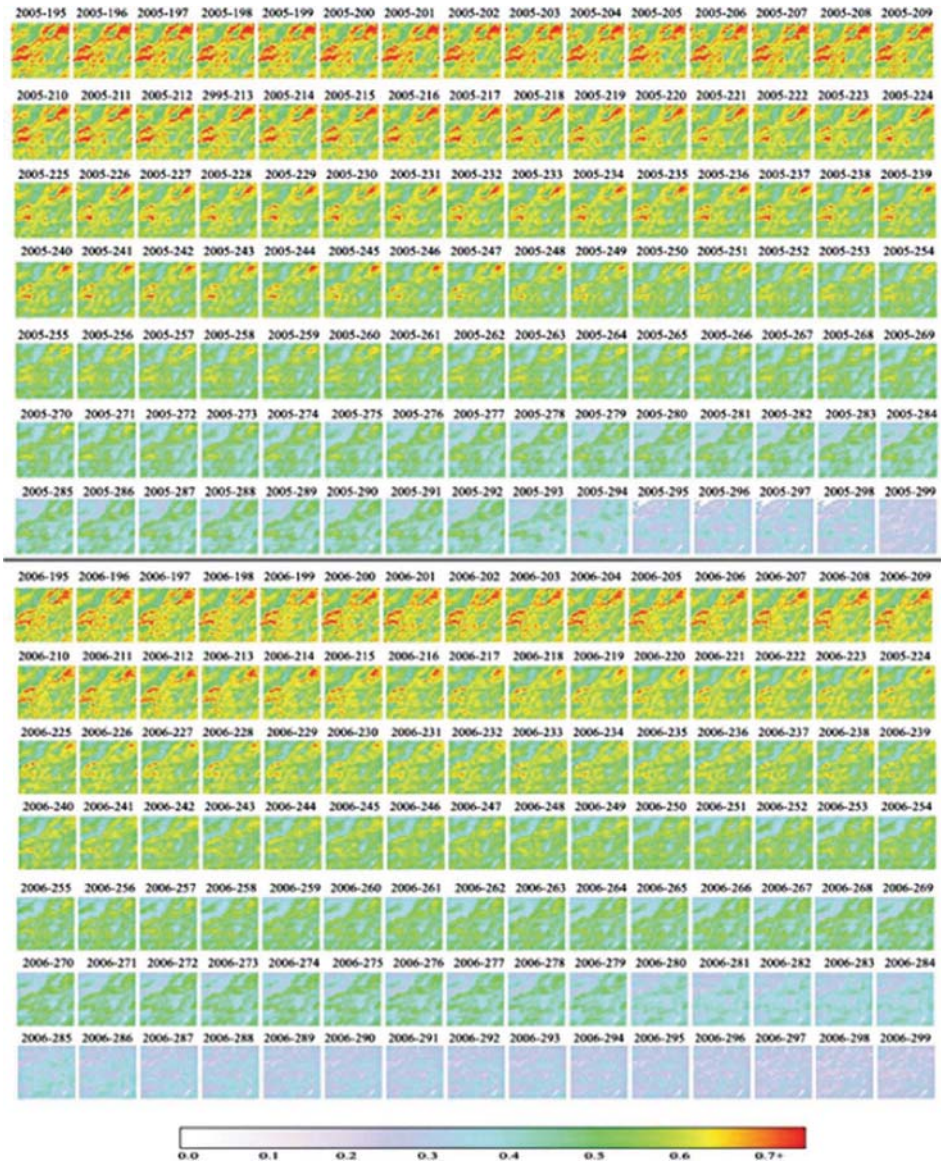

Figure 7. Temporal EVI of the small area (30 km by 30 km) centred on the Bartlett site for the year 2005 (pictures above the dark line) and for the year 2006 (pictures under the dark line).

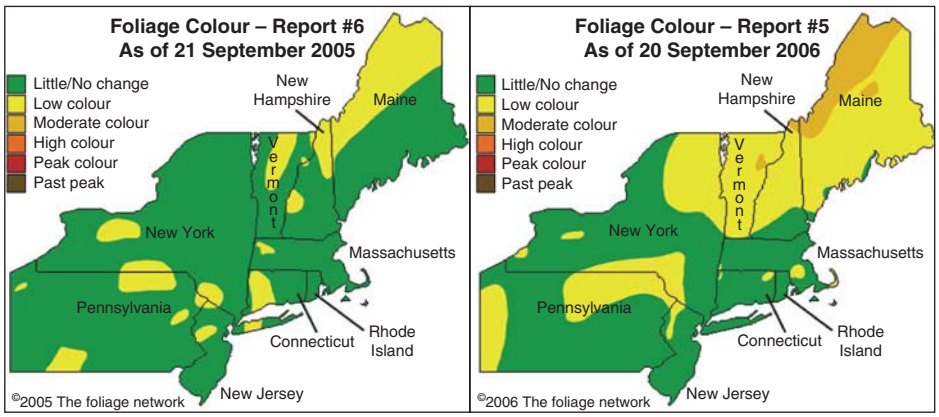

Figure 8. Ground foliage colour archived reports over the Northeast US on 21 September 2005 (left) and 20 September 2006 (right), reproduced with permission from http://www.foliagenetwork.net.

season of year 2005 progressed more slowly than year 2006, especially in northern New England (Figure 8). Warmer temperatures and a lack of summer rain in 2005 delayed the onset of fall colour (http://www.wunderground.com) to about day 264, with low colour beginning around day 274, peak foliage occurring around day 288, and the region lapsing into dormancy or past peak by day 299. These transition dates occurred about 10 days earlier during the 2006 foliage season.

3.4. Capturing subtle details by monitoring the daily NBAR-EVI

The detailed signal of the daily NBAR-based EVI plots reveals the potential of MODIS 500 m DB products to capture the natural transition of vegetation phenological events, especially for plants that have short phenological cycles, such as crops and some orchards. Clearly, subtle increases and decreases are revealed in the daily plots for the winter wheat and the almond orchards. For instance, light pink almond flowers quickly developed in the 'popcorn-bloom and petal fall' stage and temporarily shaded and retarded the signal of the green leaves. However, this induced only a 2.5% relative decrease in the EVI value during a 1 month period. Therefore, the absolute EVI change (~0.005) of this period is fairly stable as compared with the more impressive total absolute EVI change (0.224) from dormant to late nut development stage (Table 2). Such subtle variations are only revealed when the daily temporal signature is monitored.

Table 2 shows the length and maximum and minimum EVI values of each individual growth phase (determined by the fieldwork) for the three case study sites, as well as the relative variation in EVI expressed as a percentage. Various rates of EVI change are driven by different plant varieties, by different growth periods, or by different growth cycles for a given plant variety (Table 2). Compared with the tiny 2.5% relative change over 25 days during the 'popcorn bloom–petal fall' stage for the almond orchard, the jacket stage gained a dramatic 57.9% relative EVI change in a 36 day period along with the rapid development of green leaves and nuts (Table 2(A)). While the winter wheat at the Yucheng site went through its entire growth cycle from emergence to harvest within only about 130 days, with the fastest EVI increase occurring during the approximately 12 day '1st node visible' period and the greatest decrease occurring during the 2 week 'milky ripe' period, according to the foliage reports for the Northeast US in years 2005 and 2006, the major EVI

Table 2. Statistics of each growth period from the changes in the NBAR-based EVI for the California orchard (A), Yucheng winter wheat (B), and Bartlett mixed forest (C and D).

Study site	Growth phase	Days	Maximum value	Minimum value	Relative variation*
Variation of EVI for California almond orchard during 2006-001–160 (A)	Dormant stage	29	0.2347	0.2080	11.8%
	Green tip and pink bud stage	13	0.2449	0.2131	14.1%
	Popcorn, bloom, and petal fall	25	0.2467	0.2411	2.5%
	Jacket stage	36	0.3828	0.2523	57.9%
	Late nuts developing stage	57	0.4336	0.3682	29.0%
Variation of EVI values for Yucheng winter wheat during 2006-060–180 (B)	Tiller	15	0.1536	0.1434	3.1%
	Turning green	7	0.1609	0.1535	2.3%
	Erect growth	16	0.2508	0.1611	27.4%
	First node visible	12	0.3872	0.2458	43.2%
	Boot stage	13	0.4229	0.3787	13.5%
	Heading	5	0.4618	0.4229	11.9%
	Beginning flower	5	0.4640	0.4554	2.6%
	Ripening	10	0.4705	0.4496	6.4%
	Milky ripe	15	0.4406	0.3181	37.5%
	Mealy ripe	6	0.3182	0.2612	17.4%
	Kernel hard	3	0.2565	0.2374	5.8%
	Harvest	14	0.2374	0.1905	14.3%
Variation of EVI for Bartlett mixed forest during 2005-200–320 (C)	Maturity	65	0.6585	0.5344	24.4%
	Senescence	26	0.5326	0.3294	63.7%
	Dormancy	30	0.3284	0.1496	9.3%
Variation of EVI for Bartlett mixed forest during 2006-200–320 (D)	Maturity	38	0.6650	0.5404	27.2%
	Senescence	58	0.5516	0.2275	70.8%
	Dormancy	25	0.2542	0.2071	10.3%

Note: *Relative variation means the relative percent of EVI changes for each individual growth stage to the change of EVI values in the entire study period for the target plant.

decreases occurred during the senescence stage, with 63.7% and 70.8% relative change, respectively, in the foliage colour change period from days 200 to 320. But, as revealed by the daily NBAR-EVI, the start of senescence in year 2006 occurred much earlier than in 2005 because of the weather, temperature, and rain stress conditions.

The Collection V005 operational NBAR product (MCD43A4) is only retrieved once every 8 days due to archival constraints. While this frequency can usually be used to successfully capture general phenological events, it lacks the temporal frequency to monitor these more subtle variations. Furthermore, daily retrievals (which still use multi-temporal observations to inform the retrieval but emphasize the observations from a single date), may provide additional monitoring information by occasionally obtaining glimpses of the vegetation growth even during cloudier periods of the year. When a piecewise logistic function of time (Zhang et al. 2003) is fitted via non-linear least squares to the 8 day operational MODIS NBAR-EVI data available for each of the case studies, the first-order trend of EVI change and the major transition dates are generally captured. However, various subtle details in some special growth stages may be missed or smoothed out in the curve-fitting process (Figure 9). For instance, intrinsic photosynthetic activities such as the blooming

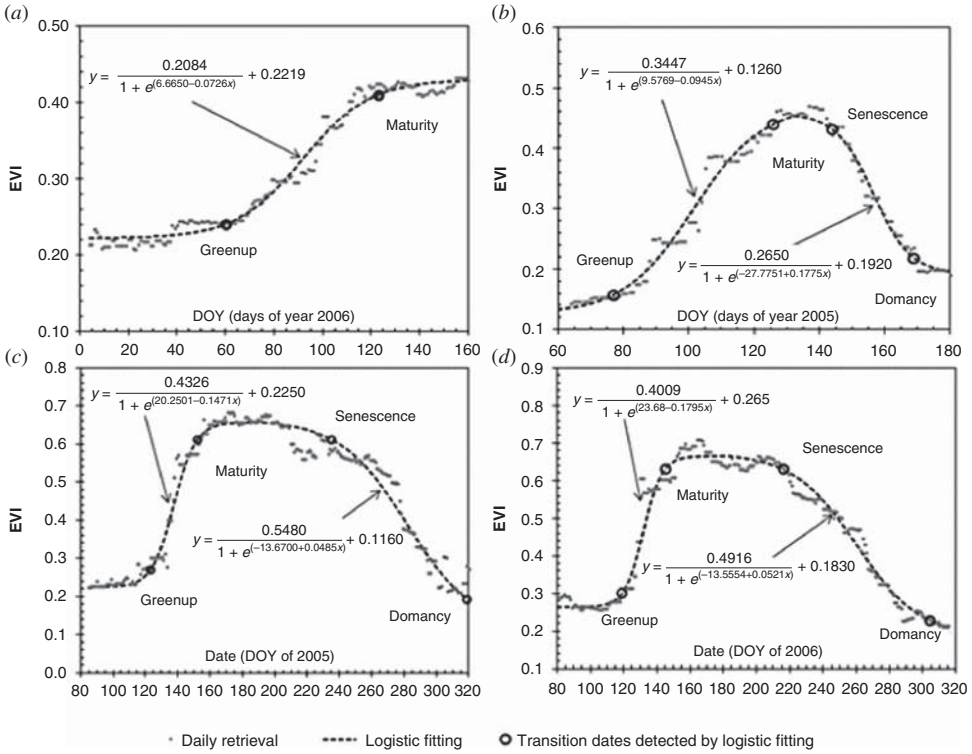

Figure 9. Comparison of daily NBAR-based EVI (grey dots) with the daily-EVI logistic fitted curve (dark-dashed lines) and the detected phenophase transition dates (empty circle) for 2006 California almond orchard (*a*), 2005 Yucheng winter wheat (*b*), and 2005 and 2006 Bartlett mixed forest (*c*) and (*d*).

period (days 40–60) of the almond orchard, the flowering period of the winter wheat, and the multiple local peaks in maturity (possibly induced by the variety of vegetation species) in the mixed forest are not captured by the logistic trends. Furthermore, the difference in timing of senescence between 2005 and 2006 is somewhat masked by the logistic fits.

4. Summary and conclusion

This study investigates the ability to detect the natural variation of vegetation phenological events, using the daily MODIS 500 m reflectance anisotropy products generated by the daily MODIS DB algorithm. The daily MODIS 500 m reflectance anisotropy products are employed to retrieve daily VIs for winter wheat in northeast China, for an almond orchard in California, and for a deciduous forest region in Bartlett, New Hampshire. Field-based measurements, including frequent field specification of surface phenology information at the Yucheng experimental site and the California almond orchard, as well as subjective estimates from local citizen scientists and webcam photos of Bartlett Forest, were acquired. Compared with these ground records, the VI trajectories derived from the daily MODIS NBAR products capture not only the detailed footprint and principal attributes of the phenological events (such as flowering, blooming) but also the substantial inter-annual variability. These studies indicate the potential for real-time monitoring of phenological events,

especially at the regional spatial scale. The MODIS instruments onboard the Terra and Aqua platforms provide a DB downlink for real-time and rapid-response monitoring. This daily NBAR product was developed for the DB community and, along with other MODIS L1B and L2G science production software, is distributed via the IMAPP (International MODIS/AIRS Processing Package) available from http://cimss.ssec.wisc.edu/imapp/.

Through these daily DB products, the link between traditional ground-based measurements and satellite-based retrievals can be further investigated to improve our understanding of phenological phase and the biological life-cycle events in vegetation. Note that any satellite-based phenology algorithm performs over the pixel scale with a mixture of various biomes, while the ground measurements for particular individual vegetation species often record specific phenology events, such as the emergence of crops, bud burst, or flowering. Thus, future research must be focused on understanding exactly how landscape-scale phenological events dominate the signal in moderate-resolution satellite pixels (Liang and Schwartz 2009). Furthermore, the possible presence of residual aerosol, cloud contamination, or snow will induce additional variation to the satellite-based observations and must be acknowledged. However, despite these caveats, these case studies demonstrate the utility of the daily MODIS DB albedo, NBAR, and BRDF products. Therefore, given these results, the 500 m MODIS Collection V006 reprocessing will also be accomplished on a daily basis, improving the global community's efforts to monitor vegetation phenology. The detailed work here focused on specific locations and specific dates mainly to demonstrate the concept and address the main objective of the article to examine the utility of the daily MODIS 500 m reflectance anisotropy DB product for monitoring the evolution of vegetation phenological trends. Further work could include extending the use of the DB product for regional and global analysis for the entire time series of MODIS data.

Acknowledgements

This work was supported by NASA NNX08AE94A. The authors would like to thank researchers at the YCES (Yucheng Experiment Station, Chinese Academic Sciences (CAS)), contributors to the blue diamond website (http://www.bluediamond.com/applications/in-the-field), contributors to the foliage network (http://www.foliagenetwork.net), researchers at the Bartlett Experiment Forest site for providing the ground phenology information, and a thorough and thoughtful review of the manuscript by Jesslyn Brown, US Geological Survey. Dr Donghui Xie acknowledges support from the open funding programme of the State Key Laboratory of Remote Sensing Science (#OFSLRSS201102). Dr Andrew D. Richardson acknowledges support from the National Science Foundation, through the Macrosystems Biology programme, award EF-1065029; the Northeastern States Research Cooperative; and the US Geological Survey Status and Trends Program, the US National Park Service Inventory and Monitoring Program, and the USA National Phenology Network through grant number G10AP00129 from the US Geological Survey. Any use of trade, product, or firm names is for descriptive purposes only and does not imply endorsement by the US Government.

References

Badhwar, G. D. 1984. "Use of LANDSAT-Derived Profile Features for Spring Small-Grains Classification." *International Journal of Remote Sensing* 5: 783–797.

Box, J. E., D. H. Bromwich, B. A. Veenhuis, L. S. Bai, J. C. Stroeve, J. C. Rogers, K. Steffen, T. Haran, and S.-H. Wang. 2006. "Greenland Ice Sheet Surface Mass Balance Variability (1988–2004) from Calibrated Polar MM5 Output." *Journal of Climate* 19: 2783–2800.

Busetto, L., R. Colombo, M. Migliavacca, E. Cremonese, M. Meroni, M. Galvagno, M. Rossini, C. Siniscalco, U. Morra Di Cella, and E. Pari. 2010. "Remote Sensing of Larch Phenological Cycle and Analysis of Relationships with Climate in the Alpine Region." *Global Change Biology* 16: 2504–2517. doi:10.1111/j.1365–2486.2010.02189.x.

Cannell, M. G. R., and R. I. Smith. 1983. "Thermal Time, Chill Days, and Prediction of Budburst in *Picea Sitchensis*." *Journal of Applied Ecology* 20: 951–963.

Cleland, E. E., I. Chuine, A. Menzel, H. A. Nooney, and M. D. Schwartz. 2007. "Shifting Plant Phenology in Response to Global Change." *Trends in Ecology and Evolution* 22: 357–365.

Cook G. D., and R. G. Heerdegen. 2001. "Spatial Variation in the Duration of the Rainy Season in Monsoonal Australia." *International Journal of Climatology* 21: 1723–1732.

de Beurs, K. M., and G. M. Henebry. 2008. "Northern Annular Mode Effects on the Land Surface Phenologies of Northern Eurasia." *Journal of Climate* 21: 4257–4279.

de Beurs, K. M., and G. M. Henebry. 2010. "Spatio-Temporal Statistical Methods for Modeling Land Surface Phenology." In *Phenological Research, Chapter 9: Methods for Environmental and Climate Change Analysis*, edited by I. L. Hudson and M. R. Keatley, 177–208. Dordrecht: Springer.

Ganguly, S., M. Friedl, B. Tan, X. Zhang, and M. Verma. 2010. "Land Surface Phenology from MODIS: Characterization of the Collection 5 Global Land Cover Dynamics Product." *Remote Sensing of Environment* 114: 1805–1816. doi:10.1016/j.rse.2010.04.005.

Heidinger, A., C. Cao, and J. Sullivan. 2002. "Using Moderate Resolution Imaging Spectrometer (MODIS) to Calibrate Advanced Very High Resolution Radiometer Reflectance Channels." *Journal of Geophysical Research* 107 (D23): AAC 11-1–AAC 11-10. doi:10.1029/2001JD002035.

Huete, A., K. Didan, T. Miura, E. P. Rodriguez, X. Gao, and L. G. Ferreira. 2002. "Overview of the Radiometric and Biophysical Performance of the MODIS Vegetation Indices." *Remote Sensing of Environment* 83: 195–213.

Hufkens, K., M. Friedl, O. Sonnentag, B. H. Braswell, T. Milliman, and A. D. Richardson. 2012. "Linking Near-Surface and Satellite Remote Sensing Measurements of Deciduous Broadleaf Forest Phenology." *Remote Sensing of Environment* 117: 307–321. doi:10.1016/j.rse.2011.10.006.

Jenkins J. P., A. D. Richardson, B. H. Braswell, S. V. Ollinger, D. Y. Hollinger, and M.-L. Smith. 2007. "Refining Light-Use Efficiency Calculations for a Deciduous Forest Canopy Using Simultaneous Tower-Based Carbon Flux and Radiometric Measurements." *Agricultural and Forest Meteorology* 143: 64–79.

Jolly, W. M., R. Nemani, and S. W. Running. 2005. "A Generalized, Bioclimatic Index to Predict Foliar Phenology in Response to Climate." *Global Change Biology* 11: 619–632.

Jonsson, P., and L. Eklundh. 2004. "TIMESAT-A Program for Analyzing Time-Series of Satellite Sensor Data." *Computers & Geosciences* 30: 833–845.

Ju, J., D. P. Roy, Y. Shuai, and C. Schaaf. 2010. "Development of an Approach for Generation of Temporally Complete Daily Nadir MODIS Reflectance Time Series." *Remote Sensing of Environment* 114: 1–20.

Justice, C., E. Vermote, J. R. G. Townshend, R. Defries, D. P. Roy, D. K. Hall, V. V. Salomonson, J. L. Privette, G. Riggs, A. Strahler, W. Lucht, R. B. Myneni, Y. Knyazikhin, S. W. Running, R. R. Nemani, Z. M. Wan, A. R. Huete, W. van Leeuwen, R. E. Wolfe, L. Giglio, J. P. Muller, P. Lewis, and M. J. Barnsley. 1998. "The Moderate Resolution Imaging Spectroradiometer (MODIS): Land Remote Sensing for Global Change Research." *IEEE Transactions on Geoscience and Remote Sensing* 36: 1228–1249.

Justiniano, M. J., and T. S. Fredericksen. 2000. "Phenology of Tree Species in Bolivian Dry Season." *Biotropica* 32: 1228–1249.

Kramer, K., I. Leinomen, and D. Loustau. 2000. "The Importance of Phenology for the Evaluation of Impact of Climate Change on Growth of Boreal, Temperate and Mediterranean Forest Ecosystems: An Overview." *International Journal of Biometeorology* 44: 67–75.

Kross, A., R. Fernandes, J. Seaquist, and E. Beaubien. 2011. "The Effect of the Temporal Resolution of NDVI Data on Season Onset Dates and Trends across Canadian Broadleaf Forests." *Remote Sensing of Environment* 115: 1564–1575.

Leroy, M., and O. Hautecoeur. 1999. "Anisotropy-Corrected Vegetation Indexes Derived from POLDER/ADEOS." *IEEE Transaction on Geoscience and Remote Sensing* 37: 1698–1708.

Li, X., and A. H. Strahler. 1992. "Geometric-Optical Bidirectional Reflectance Modeling of the Discrete Crown Vegetation Canopy: Effect of Crown Shape and Mutual Shadowing." *IEEE Transaction on Geoscience and Remote Sensing* 30: 276–292.

Liang, L., and M. D. Schwartz. 2009. "Landscape Phenology: An Integrative Approach to Seasonal Vegetation Dynamics." *Landscape Ecology* 24: 465–472. doi:10.1007/s10980-009-9328-x.

Liang, L., M. D. Schwartz, and S. Fei. 2012. "Photographic Assessment of Temperate Forest Understory Phenology in Relation to Springtime Meteorological Drivers." *International Journal of Biometeorology* 56: 343–355. doi:10.1007/s00484-011-0438-1.

Lobell, D. B., and C. B. Field. 2007. "Global Scale Climate-Crop Yield Relationships and the Impacts of Recent Warming." *Environmental Research Letters* 2: 014002. doi:10.1088/1748–9326/2/1/014002.

Lucht, W., and P. Lewis. 2000. "Theorectical Noise Sensitivity of BRDF and Albedo Retrieval from the EOS-MODIS and MISR Sensors with Respect to Angular Sampling." *International Journal of Remote Sensing* 21: 81–98.

Lucht, W., C. B. Schaaf, and A. H. Strahler. 2000. "An Algorithm for the Retrieval of Albedo from Space Using Semiempirical BRDF Models." *IEEE Transaction on Geoscience and Remote Sensing* 38: 977–998.

McKellip, R., R. E. Ryan, S. Blonski, and D. Prados. 2005. "Crop Surveillance Demonstration Using a Near-Daily MODIS Derived Vegetation Index Time Series." In *2005 International Workshop on the Analysis of Multi-temporal Remote Sensing Images*, 54–58. Biloxi, MI: IEEE.

Moody, A., and A. H. Strahler. 1994. "Characteristics of Composite AVHRR Data and Problems in their Classification." *International Journal of Remote Sensing* 15: 3473–3491.

Morisette, J. T., A. D. Richardson, A. K. Knapp, J. I. Fisher, E. A. Graham, J. Abatzoglou, B. E. Wilson, D. D. Breshears, G. M. Henebry, J. M. Hanes, and L. Liang. 2009. "Tracking the Rhythm of the Seasons in the Face of Global Change: Phenological Research in the 21st Century." *Frontiers in Ecology and the Environment* 7: 253–260. doi:10.1890/070217.

Myneni, R. B., F. G. Hall, P. J. Sellers, and A. L. Marshak. 1995. "The Interpretation of Spectral Vegetation Indexes." *IEEE Transactions on Geoscience and Remote Sensing* 33: 481–486.

Myneni, R. B., C. D. Keeling, C. J. Tucker, G. Asrar, and R. R. Nemani. 1997. "Increased Plant Growth in the Northern High Latitudes from 1981–1991." *Nature* 386: 698–702.

Narasimhan, R., and D. Stow. 2010. "Daily MODIS Products for Analyzing Early Season Vegetation Dynamics across the North Slope of Alaska." *Remote sensing of Environment* 114: 1251–1262.

Omotosho, J. B. 1992. "Long-Range Prediction of the Onset and End of the Rainy Season in the West African Sahel." *International Journal of Climatology* 12: 369–382.

Osborne, T. M., D. M. Lawrence, A. J. Challinor, J. M. Slingo, and T. R. Wheeler. 2007. "Development and Assessment of a Coupled Crop-Climate Model." *Global Change Biology* 13: 169–183. doi:10.1111/j.1365–2486.2006.01274.x.

Parmesan, C., and G. Yohe. 2003. "A Globally Coherent Fingerprint of Climate Change Impacts across Natural Systems." *Nature* 421: 37–42.

Reed, B., J. F. Brown, D. Vanderzee, T. R. Loveland, J. W. Merchant, and D. O. Ohlen. 1994. "Measuring Phenological Variability from Satellite Imagery." *Journal of Vegetation Science* 5:703–714.

Richardson, A. D., R. S. Anderson, M. A. Arain, A. G. Barr, G. Bohrer, G. Chen, J. M. Chen, P. Ciais, K. J. Davis, A. R. Desai, M. C. Dietze, D. Dragoni, S. R. Garrity, C. M. Gough, R. Grant, D. Y. Hollinger, H. A. Margolis, H. McCaughey, M. Migliavacca, R. K. Monson, J. W. Munger, B. Poulter, B. M. Raczka, D. M. Ricciuto, A. K. Sahoo, K. Schaefer, H. Tian, R. Vargas, H. Verbeeck, J. Xiao, and Y. Xue. 2012. "Terrestrial Biosphere Models Need Better Representation of Vegetation Phenology: Results from the North American Carbon Program Site Synthesis." *Global Change Biology* 18: 566–584. doi:10.1111/j.1365-2486.2011.02562.x.

Richardson, A. D., B. H. Braswell, D. Y. Hollinger, J. P. Jenkins, and S. V. Ollinger. 2009. "Near-Surface Remote Sensing of Spatial and Temporal Variation in Canopy Phenology." *Ecological Applications* 19: 1417–1428.

Richardson, A. D., D. Y. Hollinger, D. B. Dail, J. T. Lee, J. W. Munger, and J. O'Keefe. 2009. "Influence of Spring Phenology on Seasonal and Annual Carbon Balance in Two Contrasting New England Forests." *Tree Physiology* 29: 321–331. doi:10.1093/treephys/tpn040.

Richardson, A. D., J. P. Jenkins, B. H. Braswell, D. Y. Hollinger, S. V. Ollinger, and M.-L. Smith. 2007. "Use of Digital Webcam Images to Track Spring Green-Up in a Deciduous Broadleaf Forest." *Ecosystem Ecology* 152: 323–334.

Richardson, A. D., T. A. Black, P. Ciais, N. Delbart, M. A. Friedl, N. Gobron, D. Y. Hollinger, W. L. Kutsch, B. Longdoz, S. Luyssaert, M. Migliavacca, L. Montagnani, J. W. Munger, E. Moors, S. Piao, C. Rebmann, M. Reichstein, N. Saigusa, E. Tomelleri, R. Vargas, and A. Varlagin. 2010. "Influence of Spring and Autumn Phenological Transitions on Forest Ecosystem Productivity." *Philosophical Transactions of the Royal Society* 365: 3227–3246. doi:10.1098/rstb.2010.0102.

Ross, J. K. 1981. *The Radiation Regime and Architecture of Plant Stands*, edited by W. Junk, 392. Norwell, MA: Artech House.

Rötzer, T., R. Grote, and H. Pretzsch. 2004. "The Timing of Bud Burst and Its Effect on Tree Growth." *International Journal of Biometeorology* 48: 109–118.

Roujean, J.-L., M. Leroy, and P. Y. Deschamps. 1992. "A Bi-Directional Reflectance Model of the Earth's Surface for the Correction of Remote Sensing Data." *Journal of geophysical Research* D-97: 20455–20468.

Roy, D. P., P. Lewis, C. Schaaf, S. Devadiga, and L. Boschetti. 2006. "The Global Impact of Cloud on the Production of MODIS Bi-Directional Reflectance Model Based Composites for Terrestrial Monitoring." *IEEE Geoscience and Remote Sensing Letters* 3: 452–456.

Schaaf, C. B., F. Gao, A. H. Strahler, W. Lucht, X. Li, T. Tsang, N. C. Strugnell, X. Zhang, Y. Jin, J.-P. Muller, P. Lewis, M. Barnsley, P. Hobson, M. Disney, G. Roberts, M. Dunderdale, C. Doll, R. d'Entremont, B. Hu, S. Liang, J. L. Privette, and D. P. Roy. 2002. "First Operational BRDF, Albedo and Nadir Reflectance Products from MODIS." *Remote Sensing of Environment* 83: 135–148.

Schaaf, C. L. B., J. Liu, F. Gao, and A. H. Strahler. 2011. "MODIS Albedo and Reflectance Anisotropy Products from Aqua and Terra." In *Land Remote Sensing and Global Environmental Change: NASA's Earch Observing System and the Science of ASTER and MODIS*, Remote Sensing and Digital Image Processing Series, Vol. 11, edited by B. Ramachandran, C. Justice, and M. Abrams, 873pp. Berlin: Springer-Verlag.

Schwartz, M. D. 1998. "Green-Wave Phenology." *Nature* 394: 839–840.

Schwartz, M. D. 1990. "Detecting the Onset of Spring: A Possible Application of Phenological Models." *Climate Research* 1: 23–29.

Schwartz, M. D., R. Ahas, and A. Aasa. 2006. "Onset of Spring Starting Earlier across the Northern Hemisphere." *Global Change Biology* 12: 343–351.

Schwartz, M. D., B. C. Reed, and M. A. White. 2002. "Assessing Satellite-Derived Start-Of-Season Measures in the Conterminous USA." *International Journal of Climatology* 22: 1793–1805.

Shuai, Y. 2010. "Tracking Daily Land Surface Albedo and Reflectance Anisotropy with MODerate-Resolution Imaging Spectroradiometer (MODIS)." Diss. thesis, Department of Geography and Environment, Boston University.

Shuai, Y., C. B. Schaaf, A. H. Strahler, J. Liu, and Z. Jiao. 2008. "Quality Assessment of BRDF/Albedo Retrievals in MODIS Operational System." *Geophysical Research Letters* 35: L05407. doi:10.1029/2007GL032568.

Sonnentag, O., K. Hufkens, C. Teshera-Sterne, A. M. Young, M. Friedl, B. H. Braswell, T. Milliman, J. O'Keefe, and A. D. Richardson. 2012. "Digital Repeat Photography for Phenological Research in Forest Ecosystems." *Agricultural and Forest Meteorology* 152: 159–177. doi:10.1016/j.agrformet.2011.09.009.

Spano, D., C. Cesaraccio, P. Duce, and R. L. Zinder. 1999. "Phenological Stages of Natural Species and Their Use as Climate Indicators." *International Journal of Biometeorology* 42: 124–133.

Tan, B., J. T. Morisette, R. E. Wolfe, F. Gao, G. A. Ederer, J. Nightngale, and J. A. Pedelty. 2011. "An Enhanced TIMESAT Algorithm for Estimating Vegetation Phenology Metrics from MODIS Data." *IEEE Journal of Selected Topics in Applied Earthobservations and Remote Sensing* 4 (2): 361–371. doi 10.1109/JSTARS. 2010.2075916.

Wang, Z., C. B. Schaaf, M. J. Chopping, A. H. Strahler, J. Wang, M. O. Roman, A. V. Rocha, C. E. Woodcock, and Y. Shuai. 2012. "Evaluation of Moderate-Resolution Imaging Spectroradiometer (MODIS) Snow Albedo Product (MCD43A) over Tundra." *Remote Sensing of Environment* 117: 264–280.

White, M. A., K. M. de Beurs, K. Didan, D. W. Inouye, A. D. Richardson, O. P. Jensen, J. O'Keefe, G. Zhang, R. R. Nemani, W. J. D. van LeeuWen, J. F. Brown, A. de Wit, M. Schaepman, X. Lin, M. Dettinger, A. S. Bailey, J. S. Kimball, M. D. Schwartz, D. D. Baldocchi, J. T. Lee, and W. K. Lauenroth. 2009. "Intercomparison, Interpretation, and Assessment of Spring Phenology in North America Estimated from Remote Sensing for 1982–2006." *Global Change Biology* 15: 2335–2359. doi:10.1111/j.1365–2486.2009.01910.x.

White, M. A., and R. R. Nemani. 2006. "Real-Time Monitoring and Short-Term Forecasting of Land Surface Phenology." *Remote Sensing of Environment* 104: 43–49.

White, M. A., R. R. Nemani, P. E. Thornton, and S. W. Running. 2002. "Satellite Evidence of Phenological Differences Between Urbanized and Rural Areas of the Eastern United States Deciduous Broadleaf Forest." *Ecosystems* 5: 260–277.

White, M. A., S. W. Running, and P. E. Thornton. 1999. "The Impact of Growing-Season Length Variability on Carbon Assimilation and Evapo-Transpiration over 88 Years in the Eastern US Deciduous Forest." *International Journal of Biometeorology* 42: 139–145.

White, M. A., P. E. Thornton, and S. W. Running. 1997. "A Continental Phenology Model for Monitoring Vegetation Responses to Interannual Climatic Variability." *Global Biogeochemical Cycles* 1: 217–234.

Wofle, R. E., M. Nishihama, A. J. Fleig, J. A. Kuyper, D. P. Roy, J. C. Storey, and F. S. Patt. 2002. "Achieving Sub-Pixel Geolocation Accuracy in Support of MODIS Land Science." *Remote Sensing of the Environment* 83: 31–49.

Zhang, X., M. A. Friedl, and C. B. Schaaf. 2006. "Global Vegetation Phenology from Moderate Resolution Imaging Spectroradiometer (MODIS): Evaluation of Global Patterns and Comparison with In Situ Measurements." *Journal of Geophysical Research* 111: G04017. doi:10.1029/2006JG000217.

Zhang, X., M. A. Friedl, C. B. Schaaf, and A. H. Strahler. 2004. "Climate Controls on Vegetation Phenological Patterns in Northern Mid- and High Latitudes Inferred from MODIS Data." *Global Change Biology* 10: 1133–1145.

Zhang, X., M. A. Friedl, C. B. Schaaf, A. H. Strahler, J. C. F. Hodges, F. Gao, B. C. Reed, and A. Huete. 2003. "Monitoring Vegetation Phenology Using MODIS." *Remote Sensing of Environment* 84: 471–475.

Zhang, X., and M. D. Goldberg. 2010. "Monitoring Fall Foliage Coloration Dynamics Using Time-Series Satellite Data." *Remote Sensing of Environment* 115: 382–391. doi:10.1016/j.rse.2010.09.009.

Zhang, X., M. Goldberg, D. Tarpley, M. Friedl, J. Morisette, F. Logan, and Yu, Y. 2010. "Drought-Induced Vegetation Stress in Southwestern North America." *Environmental Research Letters* 5 (2): 024008. doi:10.1088/1748–9326/5/2/024008.

Zhang, X., M. D. Goldberg, and Y. Yu. 2012. "Prototype for Monitoring and Forecasting Fall Foliage Coloration in Real Time from Satellite Data." *Agricultural and Forest Meteorology* 158: 21–29. doi:10.1016/j.agrformet.2012.01.013.